PROCEEDINGS OF SCIENCE

Neutral pion polarizabilities from four-point functions in lattice QCD

Frank Lee,[a,*] **Walter Wilcox,**[b] **Andrei Alexandru,**[a] **Chris Culver**[c] **and Shayan Nadeem**[b]

[a] *Physics Department, The George Washington University, Washington, DC 20052, USA*
[b] *Department of Physics, Baylor University, Waco, Texas 76798, USA*
[c] *Department of Mathematical Sciences, University of Liverpool, Liverpool L69 7ZL, United Kingdom*

E-mail: fxlee@gwu.edu

We report a proof-of-principle lattice QCD simulation of the electric and magnetic polarizabilities for a neutral pion in the four-point function method. The results are based on the same quenched Wilson ensembles on a $24^3 \times 48$ lattice at $\beta = 6.0$ with pion mass from 1100 to 370 MeV previously used for a charged pion. For electric polarizability, the results are largely consistent with those from the background field method and ChPT. In contrast, there are significant differences for magnetic polarizability among the four-point function method, the background field method, and ChPT. The situation points to the important role of disconnected diagrams for a neutral pion. We elucidate a transparent quark decomposition in the four-point function method that can be used to shed light on the issue.

The 41st International Symposium on Lattice Field Theory (Lattice 2024)
July 28th - August 3rd, 2024
Liverpool, United Kingdom

*Speaker

PoS(LATTICE2024)331

1. Introduction

Electromagnetic polarizabilities are fundamental properties that encode information on the internal structure of hadrons. Understanding electromagnetic polarizabilities from first principles has been a long-term goal of lattice QCD. The standard approach is the background field method which introduces classical static electromagnetic fields to interact with quarks in hadrons. The appeal of the method lies in its simplicity: only two-point correlation functions are needed to measure the energy shift with or without the external field, which amounts to a standard calculation of a hadron's mass. The linear shift is related to dipole moments, and the quadratic shift to polarizabilities. The method is fairly robust and has been widely applied (see [1] for a recent review and a complete list of references). It has enjoyed the most success for neutral hadrons. When it comes to charged hadrons, however, the method faces new challenges. The reason is rather rudimentary: a charged particle accelerates in an electric field and exhibits Landau levels in a magnetic field. Such collective motion of the hadron is unrelated to polarizabilities and must be disentangled from the total energy shift in order to isolate the deformation energy on which the polarizabilities are defined. The Euclidean two-point correlation function no longer has a single-exponential behavior at large times. Special techniques have to be developed to analyze such functions for electric fields [2, 3] and magnetic fields [4–7].

Partly spurred by the challenges for charged particles, an alternative approach based on four-point functions in lattice QCD has received renewed interest in recent years. It offers a transparent physical picture that treats neutral and charged particles on equal footing; the latter simply having additional elastic contributions in the form of charge radii. The potential of using four-point functions to access polarizabilities has been investigated in the early days of lattice QCD [8–10]. An intermediate method based on a perturbative expansion in the background field at the action level was employed later [11], leading to the same diagrammatic structure as the standard four-functions discussed here. A reexamination of the formalism in Ref. [10] was carried out in Ref. [12] in which new formulas were derived in momentum space for electric and magnetic polarizabilities of both a charged pion and the proton. Proof-of-principle simulations applying the formulas for charged pion electric polarizability [13] and magnetic polarizability [14] have demonstrated the promise of such methods. At the same time, position-space-based four-point function simulations have also emerged for pions [15] and proton and neutron [16].

In this work, we focus on applying the four-point function method to a neutral pion. Outside lattice QCD, chiral perturbation theory (ChPT) as constrained by phenomenology provides most solid information on pion polarizabilities [17, 18]. At leading order, ChPT predicts $\alpha_E + \beta_M = 0$ for both charged and neutral pions. Specifically, $\alpha_E = -\beta_M = 3.0$ for a charged pion and $\alpha_E = -\beta_M = -0.5$ for a neutral pion in standard units of 10^{-4} fm^3. At two-loop order it gives for a neutral pion,

$$\alpha_E + \beta_M = 1.1 \pm 0.3,\ \alpha_E - \beta_M = -1.9 \pm 0.2,\ \alpha_E = -0.40 \pm 0.18,\ \beta_M = 1.5 \pm 0.27. \quad (1)$$

For a charged pion, it gives

$$\alpha_E + \beta_M = 0.16,\ \alpha_E - \beta_M = 5.7 \pm 0.1,\ \alpha_E = 2.93 \pm 0.05,\ \beta_M = -2.77 \pm 0.11. \quad (2)$$

We see significant differences (opposite signs) in polarizabilities between a neutral and a charged pion. This offers a good testing case for the four-point function method on the lattice. A comprehensive review on pion polarizabilities from non-lattice approaches and experiment can be found in Ref. [19].

2. Methodology

A matching procedure similar to Ref. [12] for a charged pion in the zero-momentum Breit frame (see Fig. 1) leads to the following formula,

$$\alpha_E = \lim_{\boldsymbol{q}\to 0} \frac{2\alpha}{\boldsymbol{q}^2} \int_0^\infty dt\; Q_{44}(\boldsymbol{q}, t), \tag{3}$$

for electric polarizability, and

$$\beta_M = \lim_{\boldsymbol{q}\to 0} \frac{2\alpha}{\boldsymbol{q}^2} \int_0^\infty dt \Big[Q_{11}(\boldsymbol{q}, t) - Q_{11}(\boldsymbol{0}, t) \Big], \tag{4}$$

for magnetic polarizability. The formulas are in discrete Euclidean spacetime but we keep the time axis continuous for notational convenience.

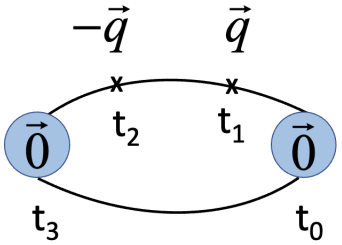

Figure 1: Zero-momentum Breit frame in Euclidean space. The four-momentum conservation is recast as $(m_\pi, \vec{0}) = (0, -\vec{q}) + (0, \vec{q}) + (m_\pi, \vec{0})$ on the lattice. The four time points are placed at t_0 (source), t_1 (current 1), t_2 (current 2), t_3 (sink).

Comparing with the formulas for a charged pion [12], there are a number of differences. For α_E, there is no elastic contribution for π_0. Both the charge radius term $\alpha\langle r_E^2\rangle/(3m_\pi)$ and Q_{44}^{elas} vanish, leading to a much simpler formula. The sign of α_E for π^0 is directly given by the sign of the time integral over Q_{44}. For β_M, the charge radius term is also absent, making its sign solely dependent on the sign of the subtracted time integral over Q_{11}. Since there is no elastic contributions for π^0, we remove the redundant 'inel' label from Q_{11}^{inel} that is used in the formula for π^+. Finally, the four-point correlation function at the quark level will be different due to the different interpolating field for a neutral pion. The four-point function is defined on the lattice by ($\mu = 1$ and 4 in this work),

$$Q_{\mu\mu}(\boldsymbol{q}, t_3, t_2, t_1, t_0) \equiv \frac{\sum_{\boldsymbol{x}_3, \boldsymbol{x}_2, \boldsymbol{x}_1, \boldsymbol{x}_0} e^{-i\boldsymbol{q}\cdot\boldsymbol{x}_2} e^{i\boldsymbol{q}\cdot\boldsymbol{x}_1} \langle\Omega|\psi(x_3) : j_\mu^L(x_2) j_\mu^L(x_1) : \psi^\dagger(x_0)|\Omega\rangle}{\sum_{\boldsymbol{x}_3, \boldsymbol{x}_0} \langle\Omega|\psi(x_3)\psi^\dagger(x_0)|\Omega\rangle}. \tag{5}$$

The interpolating field for a neutral pion is given by,

$$\psi_{\pi^0}(x) = \frac{1}{\sqrt{2}} \left[\bar{u}(x)\gamma_5 u(x) - \bar{d}(x)\gamma_5 d(x) \right]. \tag{6}$$

The resulting correlation function has self-contracting quark loops at the source and sink whereas that of a charged pion does not.

For the lattice version of electromagnetic current density j_μ^L, we consider two options. One is a local current (or Point Current) built from up and down quark fields,

$$j_\mu^{(PC)} \equiv f\ Z_V \kappa \left(q_u \bar{u}\gamma_\mu u + q_d \bar{d}\gamma_\mu d\right) \text{ with } f = \{1, i\} \text{ for } \mu = \{4, 1\}. \tag{7}$$

The extra factor of i in the magnetic case is needed to ensure that the spatial component $j_1^{(PC)}$ is hermitian. The reason is that $(\bar{u}\gamma_1 u)^\dagger = -\bar{u}\gamma_1 u$ whereas $(\bar{u}\gamma_4 u)^\dagger = \bar{u}\gamma_4 u$ (recall $\bar{u} \equiv u^\dagger\gamma_4$). The factor κ is to account for the quark-field rescaling $\psi \to \sqrt{2\kappa}\psi$ in Wilson fermions. The factor of 2 is canceled by the 1/2 factor in the definition of the vector current $\frac{1}{2}\bar{\psi}\gamma_\mu\psi$. The charge factors are $q_u = 2/3$ and $q_d = -1/3$ where the resulting $e^2 = 4\pi\alpha$ (in the unit system of $\hbar = c = \epsilon_0 = 1$) in the four-point function has been absorbed in the definition of α_E in Eq.(3) and β_M in Eq.(4). The advantage of the local operator is that it leads to relatively simple correlation functions. The drawback is the issue of renormalization constant Z_V for vector current on the lattice. The other option is the conserved vector current (or Point-Split current) for Wilson fermions,

$$\begin{aligned} j_\mu^{(PS)}(x) \equiv \quad & f\ q_u\kappa_u\big[-\bar{u}(x)(1-\gamma_\mu)U_\mu(x)u(x+\hat{\mu}) + \bar{u}(x+\hat{\mu})(1+\gamma_\mu)U_\mu^\dagger(x)u(x)\big] \\ + f\ & q_d\kappa_d\big[-\bar{d}(x)(1-\gamma_\mu)U_\mu(x)d(x+\hat{\mu}) + \bar{d}(x+\hat{\mu})(1+\gamma_\mu)U_\mu^\dagger(x)d(x)\big]. \end{aligned} \tag{8}$$

Although the conserved current explicitly involves gauge fields and leads to more complicated correlation functions, it has the advantage of circumventing the renormalization issue ($Z_V \equiv 1$). All numerical results in this work are based on conserved current.

Wick contractions of quark-antiquark pairs in $Q_{\mu\mu}$ in Eq.(5) lead to topologically distinct quark-line diagrams shown in Fig. 2. Compared to diagrams for a charged pion [13, 14], two new disconnected diagrams (G and H) emerge for a neutral pion. They are responsible for the leading $1/m_\pi$ behavior in neutral pion polarizabilities with a model-independent coefficient in ChPT [20]. The total contribution is simply the algebraic sum of the normalized individual terms,

$$Q_{\mu\mu}(\boldsymbol{q}, t_2, t_1) = \sum_{k=A,B,C,D,E,F,G,H} Q_{\mu\mu}^{(k)}. \tag{9}$$

It holds for either local current or conserved current. The charge factors and flavor-equivalent contributions have been included in each diagram. One can examine the diagrams one by one, building a transparent physical picture for the polarizabilities. For numerical results, we focus on the connected contributions (diagrams A,B,C) in the isospin limit ($\kappa_u = \kappa_d$) in this study. The disconnected contributions (diagrams D,E,F,G,H) are more challenging and are left for future work.

3. Results

As a proof-of-principle test, we use the same lattice parameters and ensembles used in Ref. [12] for a charged pion. In Fig. 3 we show in lattice units the connected contribution Q_{44} and Q_{11} at different $\boldsymbol{q}$ values as a function of current separation $t = t_2 - t_1$. Only results for $m_\pi = 600$ MeV are shown as an example; the graphs at the other pion masses look similar. The time integrals in the formulas Eq.(3) and Eq.(4) for π^0 polarizabilities are given by the shaded areas. For Q_{44}, the area is

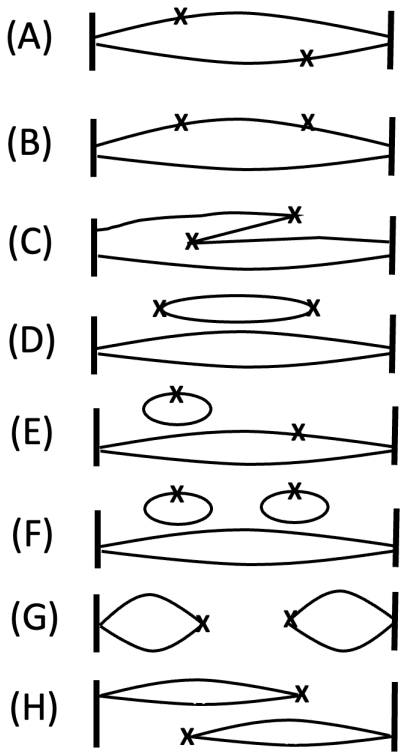

Figure 2: Quark-line diagrams of a four-point function contributing to polarizabilities of a neutral pion. Each diagram represents a distinct topology, with flavor and additional time orderings assumed as well as gluon lines that connect the quark lines. Current insertions are represented by crosses. Zero-momentum pion interpolating fields are represented by vertical bars (wall sources).

under a single curve and is positive at all $\boldsymbol{q}^2$ values. For Q_{11}, the area is from the difference between $Q_{11}(\boldsymbol{q})$ and $Q_{11}(0)$ curves, and there is a switch over of the two curves, indicating a sign change from positive to negative. Note the difference plotting scales in left and right panels: the signal is on the same order of magnitude. One detail to notice is that the curves include the $t = 0$ point which is the unphysical contact term mentioned earlier. We would normally avoid this point and only start the integral from $t = 1$. However, the chunk of area between $t = 0$ and $t = 1$ is the largest piece in the integral. To account for this contribution, we linearly extrapolated both Q_{44} and Q_{11} back to $t = 0$ using the two points at $t = 1$ and $t = 2$. As the continuum limit is approached, the $t = 0$ point will become regular and the chunk will shrink to zero.

The $\boldsymbol{q}^2$-extrapolated values as a function of pion mass are given in Fig. 4. We perform a chiral extrapolation to the physical point using two different forms. One is a polynomial form $a_0 + a_1 m_\pi + a_3 m_\pi^3$. The other is $a_0/m_\pi + a_1 m_\pi + a_3 m_\pi^3$ with a leading $1/m_\pi$ term to account for possible divergencies. The spread between the two different forms can be regarded a systematic uncertainty. Although the uncertainty from each fit is comparable, the spread is much smaller for β_M than for α_E, indicating a mild dependence on the $1/m_\pi$ term for β_M. The extrapolation leads to a sign change for α_E and the extrapolated value is consistent with that from ChPT. On the other hand the extrapolation for β_M leads to a small but positive value that is significantly smaller than that from ChPT. As a result, the sum of electric and magnetic polarizabilities $\alpha_E + \beta_M$ also tuns

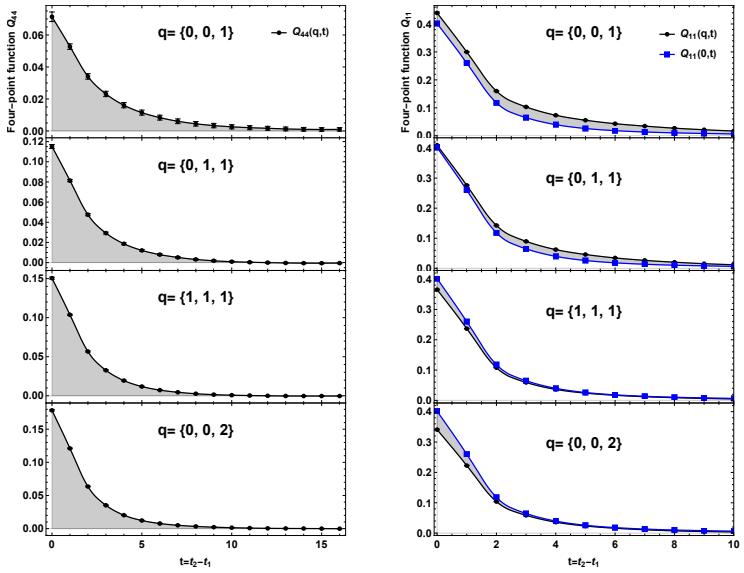

Figure 3: Connected contributions to $Q_{44}(\boldsymbol{q},t)$ (left panel) and $Q_{11}(\boldsymbol{q},t)$ (right panel) at different values of $\boldsymbol{q}$ and $m_\pi = 600$ MeV. The shaded areas are the dimensionless signal contributing to π^0 polarizabilities.

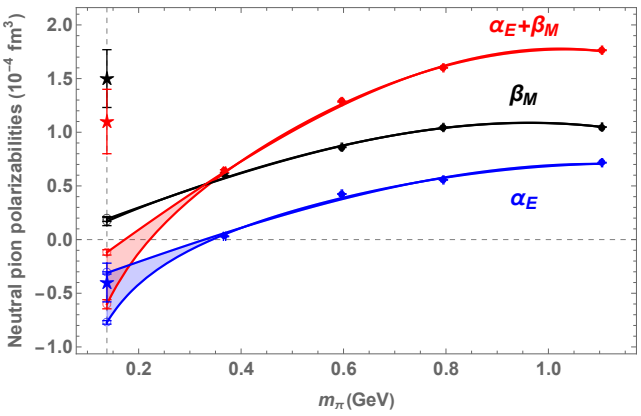

Figure 4: Chiral extrapolation of neutral pion polarizabilities. The stars at the physical point are from ChPT given in Eq.(1). The spread is from two different forms described in the text.

negative at the physical point, also at variance with ChPT.

In Fig. 5, we compare α_E from various lattice calculations in the background field method [2, 21, 22] and the four-point function method. In addition to our result in this work, there exists another study using four-point function in position space and physical pion mass [15]. By and large, the results are consistent with each other and with ChPT. So far both methods neglect disconnected contributions. Furthermore, they are electro-quenched in the sea quarks.

In contrast, the situation for β_M is rather different. We show calculations from the background field method [5, 23–27], and the sole result in the four-point function method from this work. We see large disagreements within the background field method, except Ref. [24, 26] which agree with each

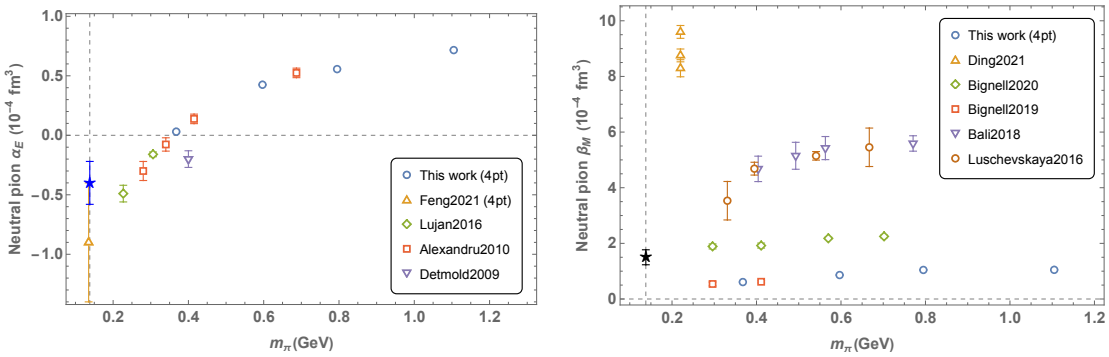

Figure 5: Neutral pion electric (left) and magnetic (right) polarizability from background field method and four-point function method (labeled by 4pt). The star at the physical point is from ChPT.

other. Notably, the four-point function result agrees with Ref. [25] but disagrees with Ref. [5] which is an improved analysis of Ref. [25] based on eigenmode projection. The situation calls for more studies in order to understand the physics mechanisms. A step in this direction is taken in Ref. [20] (also recognized in Ref. [28]) in which a chiral extrapolation of the results in Ref. [5] is performed using partially-quenched ChPT. In this approach, the neutral pion is dressed by pion cloud at various orders. It identifies the equivalent terms missing in current lattice QCD simulations and estimates the correction to be as large as 1.06 in the standard units.

We would like to mention that a potential source of systematic uncertainty among different calculations in Fig. 5 is discretization errors in the fermion action. Some of the discrepancies may be due to O(a) errors in the Wilson action and not at all related to difficulties encountered in the polarizability analysis methods.

In the four-point function formalism, we can decompose the polarizabilities into quark components. Since the formulas for π^0 in Eq.(3) and Eq.(4) are proportional to Q_{44} or Q_{11}, the relations found in the Wick contractions in the appendix directly translate to polarizabilities,

$$\alpha_E = \alpha_{uu}^{(CI)} + \alpha_{uu}^{(DI)} + \alpha_{dd}^{(CI)} + \alpha_{dd}^{(DI)} + \alpha_{ud}^{(DI)}, \tag{10}$$

$$\beta_M = \beta_{uu}^{(CI)} + \beta_{uu}^{(DI)} + \beta_{dd}^{(CI)} + \beta_{dd}^{(DI)} + \beta_{ud}^{(DI)}. \tag{11}$$

The diagonal uu and dd terms have both connected and disconnected contributions, whereas the ud cross term has only disconnected contributions (it is also absent of diagram D in Fig. 2). Furthermore, there is an exact relation between the diagonal terms,

$$\alpha_{uu}^{(CI)} = 4\alpha_{dd}^{(CI)} \text{ and } \alpha_{uu}^{(DI)} = 4\alpha_{dd}^{(DI)}, \tag{12}$$

$$\beta_{uu}^{(CI)} = 4\beta_{dd}^{(CI)} \text{ and } \beta_{uu}^{(DI)} = 4\beta_{dd}^{(DI)}. \tag{13}$$

We emphasize that the relations in Eq.(10) to Eq.(13) are specific to a neutral pion. For a charged pion, a different decomposition into charge radius, connected, and disconnected contributions exists [13, 14]. For β_M, we evaluated in this work the connected contributions $\beta_{uu}^{(CI)} + \beta_{dd}^{(CI)} = 5\beta_{dd}^{(CI)} = 0.18(2)$. If we regard the value $\beta_M = 1.50(27)$ from ChPT in Eq.(1) as the full QCD result, then the difference between ChPT and our result implies a fairly large contribution from the disconnected

diagrams $5\beta_{dd}^{(DI)} + \beta_{ud}^{(DI)} = 1.32(27)$ for π^0 magnetic polarizability. This compares well with the 1.06 estimated in Ref. [20].

4. Conclusion

A neutral pion's electromagnetic polarizabilities offer a unique opportunity to test the QCD-based methods employed to extract them. This is mainly due to the different operator structure at the quark level: $\bar{u}\gamma_5 u - \bar{d}\gamma_5 d$ for π^0 versus $\bar{d}\gamma_5 u$ for π^+. The former has self-contracting disconnected loops (see the Appendix), while the latter does not. This is true either in two-point or four-point functions.

In this work, we derived new formulas in Eq.(3) and Eq.(4) for a neutral pion in the four-point function formalism. We applied the formulas in a proof-of-concept lattice simulation using the same parameters as for a charged pion [13, 14]. The results for α_E as summarized in Fig. 5 are largely consistent with existing calculations and with ChPT. The results for β_M as summarized in Fig. 5, on the other hand, are widely inconsistent.

The situation puts a spotlight on the disconnected contributions in neutral pion magnetic polarizability. Our result from the four-point function method hints a potentially large contribution from the disconnected diagrams. It is also supported by a ChPT-based estimate [20]. Our argument is based on a straightforward decomposition of the polarizabilities in the four-point function formalism. Due to the absence of elastic contributions for π^0, the polarizabilities in Eq.(3) and Eq.(4) are proportional to the four-point functions Q_{44} and Q_{11} (albeit under time integrals). Since the four-point functions can be decomposed into quark components of various types (uu, dd, ud) according to their charge factors, the relations in the Appendix translate directly to polarizabilities as given in Eq.(10) to Eq.(13) in which connected and disconnected contributions can be further separated. Consequently, one can examine the terms one by one to see their impact on the polarizabilities. In contrast, such contributions are indirectly present via exponential or more complicated functions in the two-point functions used in the background field method.

Looking forward, the most important issue is to directly simulate the disconnected diagrams on the lattice. In the meantime, some systematic effects in the current simulation should be addressed, such as $O(a)$ scaling violations in Wilson fermions, and the quenched approximation in the gauge ensembles. Work is under way to use the $O(a)$-improved two-flavor nhyp-clover ensembles [29, 30] to repeat the analysis for both neutral and charged pions. The six dynamical ensembles described in Ref. [30] with elongated geometries also afford the opportunity to study finite-volume effects as well as to reach smaller momentum and pion mass.

Acknowledgments

This work was supported in part by U.S. Department of Energy under Grant No. DE-FG02-95ER40907 (FL, AA) and UK Research and Innovation grant MR/S015418/1 (CC). WW would like to acknowledge support from the Baylor College of Arts and Sciences SRA program. Computing resources at DOE-sponsored NERSC and NSF-sponsored TACC were used.

References

[1] G. Endrodi, *QCD with background electromagnetic fields on the lattice: a review*, 2406.19780.

[2] W. Detmold, B.C. Tiburzi and A. Walker-Loud, *Extracting Electric Polarizabilities from Lattice QCD*, *Phys. Rev. D* **79** (2009) 094505 [0904.1586].

[3] H. Niyazi, A. Alexandru, F.X. Lee and M. Lujan, *Charged pion electric polarizability from lattice QCD*, *Phys. Rev. D* **104** (2021) 014510 [2105.06906].

[4] R. Bignell, J. Hall, W. Kamleh, D. Leinweber and M. Burkardt, *Neutron magnetic polarizability with Landau mode operators*, *Phys. Rev. D* **98** (2018) 034504 [1804.06574].

[5] R. Bignell, W. Kamleh and D. Leinweber, *Pion magnetic polarisability using the background field method*, *Phys. Lett. B* **811** (2020) 135853.

[6] R. Bignell, W. Kamleh and D. Leinweber, *Magnetic polarizability of the nucleon using a Laplacian mode projection*, *Phys. Rev. D* **101** (2020) 094502 [2002.07915].

[7] F. He, D.B. Leinweber, A.W. Thomas and P. Wang, *Chiral extrapolation of the charged-pion magnetic polarizability with Padé approximant*, *Phys. Rev. D* **104** (2021) 054506 [2104.09963].

[8] M. Burkardt, J. Grandy and J. Negele, *Calculation and interpretation of hadron correlation functions in lattice qcd*, *Annals Phys.* **238** (1995) 441.

[9] W. Andersen and W. Wilcox, *Lattice charge overlap. 1. Elastic limit of pi and rho mesons*, *Annals Phys.* **255** (1997) 34 [hep-lat/9502015].

[10] W. Wilcox, *Lattice charge overlap. 2: Aspects of charged pion polarizability*, *Annals Phys.* **255** (1997) 60 [hep-lat/9606019].

[11] M. Engelhardt, *Neutron electric polarizability from unquenched lattice QCD using the background field approach*, *Phys. Rev. D* **76** (2007) 114502 [0706.3919].

[12] W. Wilcox and F.X. Lee, *Towards charged hadron polarizabilities from four-point functions in lattice QCD*, *Phys. Rev. D* **104** (2021) 034506 [2106.02557].

[13] F.X. Lee, A. Alexandru, C. Culver and W. Wilcox, *Charged pion electric polarizability from four-point functions in lattice QCD*, *Phys. Rev. D* **108** (2023) 014512 [2301.05200].

[14] F.X. Lee, W. Wilcox, A. Alexandru and C. Culver, *Magnetic polarizability of a charged pion from four-point functions in lattice QCD*, *Phys. Rev. D* **108** (2023) 054510 [2307.08620].

[15] X. Feng, T. Izubuchi, L. Jin and M. Golterman, *Pion electric polarizabilities from lattice QCD*, *PoS* **LATTICE2021** (2022) 362 [2201.01396].

[16] X.-H. Wang, Z.-L. Zhang, X.-H. Cao, C.-L. Fan, X. Feng, Y.-S. Gao et al., *Nucleon Electric Polarizabilities and Nucleon-Pion Scattering at the Physical Pion Mass*, *Phys. Rev. Lett.* **133** (2024) 141901 [2310.01168].

[17] U. Burgi, *Charged pion pair production and pion polarizabilities to two loops*, *Nucl. Phys. B* **479** (1996) 392 [hep-ph/9602429].

[18] J. Gasser, M.A. Ivanov and M.E. Sainio, *Revisiting gamma gamma —> pi+ pi- at low energies*, *Nucl. Phys. B* **745** (2006) 84 [hep-ph/0602234].

[19] M. Moinester and S. Scherer, *Compton Scattering off Pions and Electromagnetic Polarizabilities*, *Int. J. Mod. Phys. A* **34** (2019) 1930008 [1905.05640].

[20] F. He, D.B. Leinweber, A.W. Thomas and P. Wang, *Chiral extrapolation of the magnetic polarizability of the neutral pion*, *Phys. Rev. D* **102** (2020) 114509 [2010.01580].

[21] M. Lujan, A. Alexandru, W. Freeman and F.X. Lee, *Finite volume effects on the electric polarizability of neutral hadrons in lattice QCD*, *Phys. Rev.* **D94** (2016) 074506 [1606.07928].

[22] A. Alexandru and F. Lee, *Hadron electric polarizability – finite volume corrections*, *PoS* **Lattice 2010** (2011) 131.

[23] H.T. Ding, S.T. Li, A. Tomiya, X.D. Wang and Y. Zhang, *Chiral properties of (2+1)-flavor QCD in strong magnetic fields at zero temperature*, *Phys. Rev. D* **104** (2021) 014505 [2008.00493].

[24] G.S. Bali, B.B. Brandt, G. Endrődi and B. Gläßle, *Meson masses in electromagnetic fields with Wilson fermions*, *Phys. Rev. D* **97** (2018) 034505 [1707.05600].

[25] R. Bignell, W. Kamleh and D. Leinweber, *Pion in a uniform background magnetic field with clover fermions*, *Phys. Rev. D* **100** (2019) 114518 [1910.14244].

[26] E.V. Luschevskaya, O.E. Solovjeva and O.V. Teryaev, *Magnetic polarizability of pion*, *Phys. Lett. B* **761** (2016) 393 [1511.09316].

[27] E.V. Luschevskaya, O.E. Solovjeva and O.V. Teryaev, *Determination of the properties of vector mesons in external magnetic field by Quenched $SU(3)$ Lattice QCD*, *JHEP* **09** (2017) 142 [1608.03472].

[28] J. Hu, F.-J. Jiang and B.C. Tiburzi, *Pion Polarizabilities and Volume Effects in Lattice QCD*, *Phys. Rev. D* **77** (2008) 014502 [0709.1955].

[29] H. Niyazi, A. Alexandru, F.X. Lee and R. Brett, *Setting the scale for nHYP fermions with the Lüscher-Weisz gauge action*, *Phys. Rev. D* **102** (2020) 094506 [2008.13022].

[30] R. Brett, C. Culver, M. Mai, A. Alexandru, M. Döring and F.X. Lee, *Three-body interactions from the finite-volume QCD spectrum*, *Phys. Rev. D* **104** (2021) 014501 [2101.06144].